

ChemComm

Accepted Manuscript



This is an *Accepted Manuscript*, which has been through the Royal Society of Chemistry peer review process and has been accepted for publication.

Accepted Manuscripts are published online shortly after acceptance, before technical editing, formatting and proof reading. Using this free service, authors can make their results available to the community, in citable form, before we publish the edited article. We will replace this *Accepted Manuscript* with the edited and formatted *Advance Article* as soon as it is available.

You can find more information about *Accepted Manuscripts* in the [Information for Authors](#).

Please note that technical editing may introduce minor changes to the text and/or graphics, which may alter content. The journal's standard [Terms & Conditions](#) and the [Ethical guidelines](#) still apply. In no event shall the Royal Society of Chemistry be held responsible for any errors or omissions in this *Accepted Manuscript* or any consequences arising from the use of any information it contains.

COMMUNICATION

Enhanced Photocatalytic Hydrogen Evolution from Water by Niobate Single Molecular Sheets and Ensembles†

Cite this: DOI: 10.1039/x0xx00000x

Received 00th January 2012,
Accepted 00th January 2012Keizo Nakagawa,^{a,b} Tiantian Jia,^a Weiran Zheng,^a Simon Michael Fairclough,^a
Masahiro Katoh,^b Shigeru Sugiyama,^b Shik Chi Edman Tsang^{a*}

DOI: 10.1039/x0xx00000x

www.rsc.org/

We report single molecular sheets of niobate prepared by a simple bottom-up approach using hydrothermal synthesis of niobium ethoxide with the aid of triethanolamine as a structural modifier: the high kinetic stability of these molecular entities against self-assembly allows them to mix well with other colloids and facilitates their extensive electronic interactions and thus photocatalytic hydrogen evolution activity from water is much enhanced over composite of single niobate sheets with graphene and MoS₂ due to efficient electron transfer and charge separation.

Two dimensional transition metal oxide sheets,^{1,2} as a new class of nanoscale materials, offer many attractive features such as high surface areas, defined and controllable surface acidity and favorable electron-transfer characteristics, which can potentially find exciting applications as solid-acid catalysts^{3–6} and photocatalysts.^{7–14} Reduced layered niobate sheets in contact with noble metal containing cocatalysts such as Pt,^{9,11,12,14} Ru,¹⁰ Ir,¹⁴ or Rh¹³ to create Schottky barrier junctions have recently been shown to photocatalyse water splitting, which in conjunction with sunlight could constitute to a new source of clean hydrogen fuel.¹⁵ The most common synthesis method to obtain two dimensional molecular sheets from corresponding bulk layered oxide is by a top-down approach including ‘chemical vapour deposition method’ and ‘exfoliation method’.^{1–14} Typically, for the latter method, multi-layered bulk compounds can be exfoliated by first intercalating their layers with base molecules, followed by rupturing these layered structures to yield unilaminar colloids. However, the prepared colloidal molecular sheets in solution are highly unstable and would readily undergo self-restacking and precipitation if ionic strength or pH of the solution is slightly altered. In addition, this technique requires a long and cumbersome preparative procedure, including successive acid-base treatments, to yield only a small quantity of molecular sheets. Recently, a modified exfoliation method has been reported to produce a sheet-like structure of niobate under hydrothermal conditions.¹⁶ As a result, reduced layered K₄Nb₆O₁₇

with shorter preparation time was obtained. The separation of the layered structure to single molecular sheets is however not yet demonstrated. Here, we report a new bottom-up approach using a method of controlled hydrolysis and condensation of niobium ethoxide as a substrate molecule to produce single two-dimensional molecular layer of niobate in solution by hydrothermal method using triethanolamine (TEOA) as an adsorbing–chelating ligand. It is found that the molecular niobate entities prepared by this hydrothermal method give higher photo-catalytic hydrogen activity from water decomposition compared with those samples prepared by exfoliation methods. The method also allows simple and intimate assembly of the single molecular niobate sheets with graphene and MoS₂, which is found to greatly improve the hydrogen evolution activity by enhanced electron transfer and charge separation.

Single molecular layers of niobate were synthesized using hydrothermal method (see ESI) of niobium(V) ethoxide (Nb(OEt)₅) as niobium source in ammonium aqueous solution in the presence of triethanolamine (TEOA). The samples are denoted as hy-Nb-TEOA. Niobate sheets synthesized by the same method without the TEOA surfactant are denoted as hy-Nb. Structural analysis of the hydrothermal samples was carried out by TEM and AFM (**Figure 1**) and XRD (**Figure 2**). Upon inspecting the hy-Nb sample, a rolled or scrolled molecular sheets morphology was typically observed by the TEM with occasionally stacking of the sheets to a thickness of 4–20 layers with an interlayer separation of 0.89 ± 0.2 nm (ESI). In contrast, distinct flat single molecular layer sheets with sharp edges were observed in the hy-Nb-TEOA sample (**Figures 1(b)**) with only a few regions showing stacked structures with a separation of 0.84 ± 0.2 nm. **Figure 2(a)** highlights similar XRD patterns for the two samples which do not seem to correspond to any known pure niobium oxide related phases. Whilst the main diffraction peaks of both samples follow the XRD patterns of bulk HNb₃O₈ (PDF no. 37-0833), smaller diffraction peaks of niobium oxide and ammonium niobium oxide could also be present. Interestingly, the small but broad peak at 9.0° , corresponding to (020) diffraction of stacked molecular layers of [O-Nb-O] with a spacing of 0.9 ± 0.05 nm, can

be clearly seen in the case of hy-Nb sample. Scherrer analysis of this peak suggests the sample with an average thickness of about 6 molecular layers, the value of which falls within the size range observed from the TEM (ESI). In contrast, the hy-Nb-TEOA sample shows a severe broadening or nearly absence of the (020) peak implying the extremely ultrathin layered structures (an estimated thickness of less than 4 layers will cause XRD broadening of this peak rendering it almost indistinguishable from background). UV-visible absorption spectra for the two samples are shown in **Figure 2(b)**. Both samples exhibit absorption bands in the UV region (<400 nm) with the position of the absorption edge shifted to shorter wavelengths in the case of hy-Nb-TEOA sample. The calculated band-gap energies of hy-Nb and hy-Nb-TEOA correspond to 3.68 and 3.76 eV, respectively (ESI) in contrast to the multi-layered HfNb_3O_8 band gap of 3.58 eV.¹⁷ It is generally accepted that the degree of band-gap energy blue-shift due to quantum confinement in anisotropic 2D crystallite is inversely dependent on number of interlayers.¹⁸ These results clearly indicate the formation of predominant 2D layered structures for both samples. The most significant blue shifts were observed in the hy-Nb-TEOA highlighting the higher proportion of single molecular sheets than the hy-Nb sample. As a result, the average thickness of hy-Nb-TEOA sheets and their thickness distribution have been extensively characterized by AFM in the local and wide scanned regions, which showed greater than 90% of the sheets within experimental errors, are single sheet entities (see **Figure 1(c) and (d)** and ESI).

It is thus interesting to find that this hydrothermal technique can strike a control on the chemical reactions of $\text{Nb}(\text{OEt})_5$ and water to create nucleation and growth of niobium oxide as 2-D molecular sheets without their 3-D stacking. The growth of O-Nb-O networks is generally known to proceed by two main steps: hydrolysis and condensation.¹⁹ The hydrolysis and condensation of $\text{Nb}(\text{OEt})_5$ are very fast reactions (nucleophilic substitution, $\text{S}_\text{N}2$) and can proceed at once due to the large positive partial charge, δ^+ (0.53 for Nb).²⁰ In order to control the evolution of the niobium oxide structure in 2-D and morphology (e.g. sheet structure) under solution-like homogeneous conditions, TEOA is here attempted as a adsorbing-chelating ligand²¹ for $\text{Nb}(\text{OEt})_5$ which is envisaged to play a key role to stabilize of Nb against rapid hydrolysis in alkaline range. It is anticipated that the presence of this molecule can slowdown both the hydrolysis and condensation of $\text{Nb}(\text{OEt})_5$ and reduce the rapid crystal growth. As a result, anionic niobate consisting of a NbO_6 octahedral framework is first formed with the access of abundant OH^- under basic conditions. A molecular layered niobate sheet would be gradually constructed in form of $\text{NH}_4\text{Nb}_3\text{O}_8$ by packing the anionic NbO_6 monolayer with NH_4^+ from the added NH_4OH solution. During the synthesis process, cation exchange proceeds and the final HfNb_3O_8 like molecular layer would be produced. In the case of hy-Nb-TEOA, the single molecular layer sheets can be stabilized against stacking in the presence of TEOA as strong surface adsorbate molecules. Thus, they would reduce the stacking of molecular layers as the 3-D structure. Notice that the solid product was apparently covered with organic compounds even after washing with distilled water (TGA in ESI). We believe the facilitated formation of high quality and quantity of 2-D niobate molecular layers produced by this method is important which may lead to

understanding of photocatalytic chemistry on a molecular level, and would shed light on rational design, synthesis, assembly and more effective applications of photocatalysts.

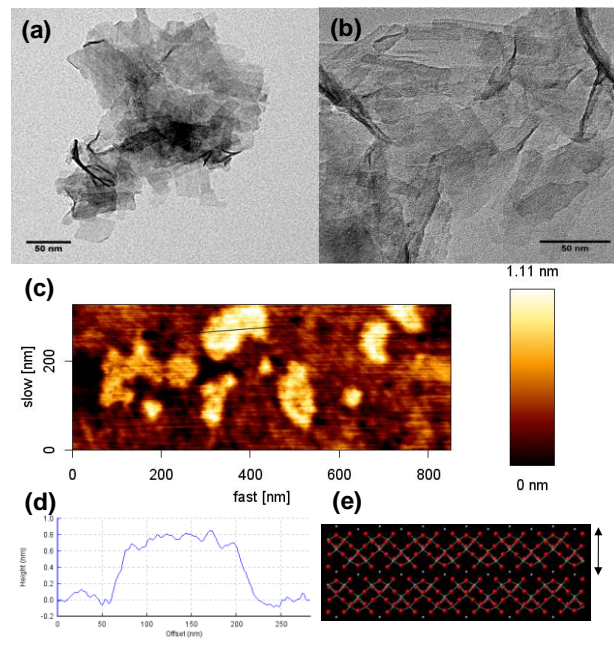


Figure 1. (a) TEM image of hy-Nb-TEOA; (b) HRTEM image of discrete hy-Nb-TEOA single molecular sheets; (c) AFM image of hy-Nb-TEOA, (d) a thickness evaluation of hy-Nb-TEOA sheets by atomic force microscopy (c) and (e) Height profile of a hy-Nb-TEOA sheet and corresponding single molecular layer dimension of HfNb_3O_8 (atomic model). Atoms are color labeled as follows: Nb (green), H (white) and O (red): this image of which was generated by Crystal Maker based on the H substitution of KNb_3O_8 . Arrow shows the thickness of the HfNb_3O_8 monolayer of 0.9nm.

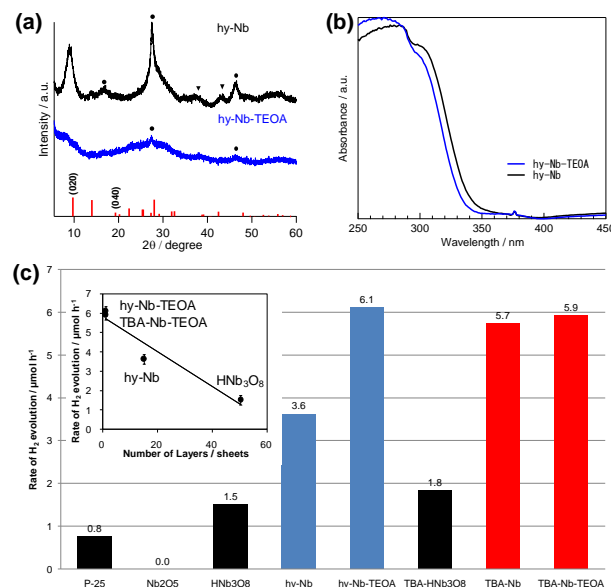


Figure 2. (a) XRD of hy-Nb and hy-Nb-TEOA. Red lines: HfNb_3O_8 (PDF no. 37-0833), \blacktriangledown : NbO (PDF no. 12-0607), \bullet : $(\text{NH}_4)_3\text{Nb}_3\text{O}_8$ (PDF no. 17-0589); (b) UV-vis absorption spectra of hy-Nb and hy-Nb-TEOA; (c) Photocatalytic hydrogen evolutions of P-25, Nb_2O_5 , HfNb_3O_8 , hy-Nb, hy-Nb-TEOA, TBA- HfNb_3O_8 , TBA-Nb and TBA-Nb-TEOA (20mg samples in 10% $\text{CH}_3\text{OH}/\text{H}_2\text{O}$); insert: hydrogen evolution versus number of layer for niobate samples.

As a result, initial photocatalytic hydrogen evolution activities from water splitting of the prepared samples were evaluated in water under UV lamp excitation (280–320 nm, 500 W) using methanol as a sacrificial reagent (**Figure 2(c)**). Control testing of low surface areas commercial Degussa P-25 (standard TiO_2 sample) and Nb_2O_5 (Johnson Matthey) powders as compared to a synthesized HfNb_3O_8 sample by using conventional calcination followed by acid treatments according to previous reports²² were carried out. Notice that layered niobium oxides have been reported to be active for photocatalysis for water splitting.^{7–14} Indeed, our partially dispersed layered HfNb_3O_8 structure (ca. 50 layers estimated from TEM/AFM images) produced higher amount of hydrogen from water than the P-25 and Nb_2O_5 suspension powders even it has a lower surface area. Comparatively, niobate sheets prepared by hydrothermal method (hy-Nb with 15 layers), purified and re-dispersed in test solution showed a much higher photocatalytic activity with a hydrogen production rate of $3.6 \mu\text{mol h}^{-1}$. Interestingly, the TEOA modified niobate molecular sheets (hy-Nb-TEOA, which are mostly single layers as shown in TEM/AFM images), gave the highest hydrogen evolution rate of $6.1 \mu\text{mol h}^{-1}$. The hydrogen evolution activities against the number of layers for each niobate samples are shown in the **insert of Figure 2(c)**. Whilst some errors in the estimations of numbers of layer based on XRD, TEM and AFM measurements exist (ESI), the trend of higher hydrogen productivity with smaller numbers of layer is for the first time clearly evident from this work. We attribute the improved photo-catalysis of the 2D structures with reduced thickness over bulkier forms to the combination of at least three factors. First, the increase in surface to volume ratio of sample would favor thinner layers for higher hydrogen activity per gram basis (20mg) although the activity did not seem to straightly proportion to their surface area (see surface areas values in ESI). Secondly, the produced electrons and holes (excitons) from the inner structure would have to diffuse to surface for photocatalysis, their long diffusion paths and recombination over structural defects would be key issues.¹⁴ Thirdly, we believe that the conduction band edge potential of this semiconductor oxide is also an important parameter in the H_2 production rate from water. For H_2 evolution from water splitting the conduction band edge should lie at a potential more negative than the water reduction potential ($< 0\text{V}$ vs. NHE at pH 0). We have estimated the conduction band potentials for hy-Nb, hy-Nb-TEOA and HfNb_3O_8 from their band-gap energies^{12,23} as shown in Table S1. As a result, the potential of the conduction band edge for hy-Nb-TEOA is more negative than those for hy-Nb and HfNb_3O_8 , suggesting an additional driving force for the water reduction. The precise contributions of the three factors are not yet known.

As stated, the common top down approach using exfoliation method is also well known to generate single molecular entity sheets although a cumbersome technique is used. Improved photochemical properties of layered niobate by exfoliation process using TBAOH have been demonstrated.^{9,11,14} As a result, exfoliated colloidal solutions including hy-Nb and hy-Nb in the presence of TEOA as a base encoded as TBA-Nb and TBA-Nb-TEOA, respectively were prepared according to the stepwise procedure.^{11,14} In addition, for comparative purposes, the colloidal sample of bulkier HfNb_3O_8 was also prepared in TBA and is denoted as TBA- HfNb_3O_8 (ESI). The samples were evaluated for photocatalytic hydrogen evolution

(**Figures 2(c) insert**). It was found that the hydrogen production activity for multilayered HfNb_3O_8 with and without TBA was similar. However, the activities of TBA-Nb and TBA-Nb-TEOA samples prepared by exfoliation were only marginally lower than the hy-Nb-TEOA within $\pm 0.5 \mu\text{mol h}^{-1}$ errors. Indeed, TEM characterization clearly showed single molecular layer niobate sheets for TBA-Nb and TBA-Nb-TEOA samples (**Figure S4b**) with similar band edge value as hy-Nb-TEOA sample (ESI). The marginal reduction in activity could be attributed to a mild blockage of surface sites by the adsorption of bulkier TBA^+ cations with negatively charged molecular sheets through electrostatic means.^{11,14} It is clear that both exfoliation and hydrothermal techniques can produce single molecular Nb sheets in solution. However, in photocatalysis, it is generally known that upon light excitation, the majority of produced excitons in the semiconductor oxide including the Nb oxide will readily recombine on a very short timescale to release heat or electromagnetic radiation before surface redox chemical reactions to take place. To enhance the lifetime of the charge carriers for redox reactions it was thought that coating or depositing with other semiconductors to form heterojunction structures in which fast charge separation could occur would prolong the excitons lifetime, hence improving the hydrogen productivity. Graphene (Gr) and MoS_2 have similarly layered structures and can also be dispersed in solution to enable a good and close contact to the niobate sheets with different potential energies. They are characterized with interesting electron mobility and optical properties.^{24–29} Thus, the single niobate molecular sheets prepared by hydrothermal method were added to graphene or MoS_2 by simple physical mixing in powder forms before re-dispersion in test solutions (TEM images in ESI). It is noted that catalytic controls of graphene and MoS_2 were found to be inert for photocatalytic hydrogen production (**Figure 3**). It is very interesting to find that, upon introduction of graphene and MoS_2 , a dramatic improvement in photocatalytic hydrogen production activity was clearly noted. The measured hydrogen evolution rates for hy-Nb-TEOA+Gr, hy-Nb-TEOA+ MoS_2 and hy-Nb-TEOA+Gr+ MoS_2 of 15.2, 28.1 and $42.4 \mu\text{mol h}^{-1}$ respectively were many folds higher than that of hy-Nb-TEOA, the significance of the results has not been realized previously. In contrast, attempts to use TBA stabilized niobate sheets prepared by exfoliation method in strong base were unsuccessful due to the unstable dispersions with graphene and MoS_2 , which led to precipitation.

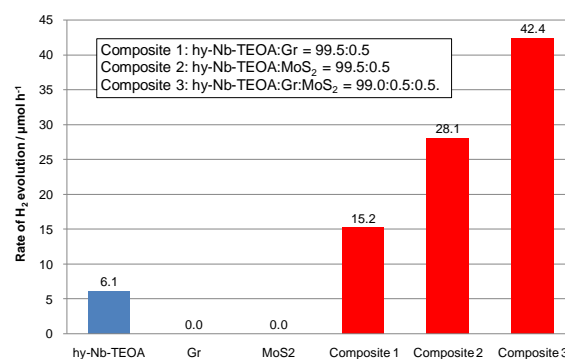


Figure 3. Adding graphene and MoS_2 to hy-Nb-TEOA by physical mixing for photocatalytic hydrogen evolution rates (20mg samples in 10% methanol)

Thus, in this work we have clearly demonstrated that the intimate assembly of molecular niobate sheets prepared by hydrothermal method with inexpensive non-precious metal layered structures such as graphene and MoS₂ can give highly effective composite for photo-generation of hydrogen from water. By using time-resolved photo-luminescence (PL) spectroscopy we have shown earlier that a fast electron transfer can be established between MoS₂ and graphene of a similar layered structure.²⁸ MoS₂ has a lower conduction band position than those of niobate but its edge sites can offer lower activation energy for H₂O reduction while conjugated graphene structure may act as electron transfer mediator.^{24,27,28} In the test mixture, it is anticipated that the 2D niobate molecular sheets absorb light and generate excited electrons and holes under UV irradiation.^{7–14} While the holes are scavenged by a sacrificial reagent (methanol), a rapid electron transfer from niobate nanosheets to MoS₂ through the two-dimensional carbon nanosheets must reduce the rate of recombination of electron-hole pairs in niobate molecular sheets and facilitates the catalytic hydrogen production on the MoS₂ edge sites through a fast photoelectron excitation between the hetero-structures (Figure S15). It is thus important to present graphene and MoS₂ in a very close proximity to the single layer niobate sheets without blocking their catalytically active sites so efficient ensembles can be established. Our results clearly highlight that the hydrothermal method to generate single molecular hy-Nb-TEOA sample is well suited for this purpose. As a result, the ensemble leads to the unprecedented improvement in the separation of photogenerated electron-hole pairs, effectively prolonging the lifetime of charge carriers, enlarging reaction zone, and consequently enhancing photocatalytic activity for hydrogen evolution.

Conclusion

In summary, we have demonstrated that single molecular layer niobate sheets in the presence of triethanolamine can be effectively prepared by hydrothermal method. As a result, it also facilitates the assembly with graphene and MoS₂ as homogeneous dispersion in a simple physical mixture. These novel sheets composites are shown to be active for effective photocatalytic production of hydrogen from water.

Notes and references

^a KN, TJ, WZ, SMF, * SCET, Department of Chemistry, University of Oxford, OX1 3QR, UK; E-mail: edman.tsang@chem.ox.ac.uk

^b KN, MK, SS, Department of Advanced Materials, Institute of Technology and Science, Tokushima University, Tokushima 770-8506, Japan

Electronic Supplementary Information (ESI) available: See DOI: 10.1039/c000000x/

1. R. Schaak and T. E. Mallouk, *Chem. Mater.*, 2000, **12**, 2513–2516.
2. T. Sasaki, S. Nakano, S. Yamauchi, and M. Watanabe, *Chem. Mater.*, 1997, **9**, 602–608.
3. A. Takagaki, M. Sugisawa, D. Lu, J. N. Kondo, M. Hara, K. Domen, and S. Hayashi, *J. Am. Chem. Soc.*, 2003, **125**, 5479–5485.
4. A. Takagaki, D. Lu, K. N. Hara Michikazu, S. Hayashi, and K. Domen, *Chem. Mater.*, 2005, **17**, 2487–2489.
5. A. Dias, S. Lima, D. Carriazo, V. Rives, M. Pillinger, and A. A. Valente, *J. Catal.*, 2006, **244**, 230–237.
6. Y. Zhao, X. Zhou, L. Ye, and S. Tsang, *Nano Rev.*, 2012, **3**, 17631–17641.
7. A. Kudo, A. Tanaka, K. Domen, K. Maruya, K. Aika, and T. Onishi, *J. Catal.*, 1988, **111**, 67–76.
8. R. Abe, K. Shinohara, A. Tanaka, M. Hara, J. N. Kondo, and K. Domen, *Chem. Mater.*, 1997, **9**, 2179–2184.
9. Y. Ebina, T. Sasaki, M. Harada, and M. Watanabe, *Chem. Mater.*, 2002, **14**, 4390–4395.
10. Y. Ebina, N. Sakai, and T. Sasaki, *J. Phys. Chem. B*, 2005, **109**, 17212–17216.
11. O. Compton, E. Carroll, J. Y. Kim, D. S. Larsen, and F. E. Osterloh, *J. Phys. Chem. C*, 2007, **111**, 14589–14592.
12. K. Maeda and T. E. Mallouk, *J. Mater. Chem.*, 2009, **19**, 4813–4818.
13. Y. Okamoto, S. Ida, J. Hyodo, H. Hagiwara, and T. Ishihara, *J. Am. Chem. Soc.*, 2011, **133**, 18034–1803.
14. E. Sabio, R. Chamousis, N. D. Browning, and F. E. Osterloh, *J. Phys. Chem. C*, 2012, **116**, 3161–3170.
15. A. Fujishima and K. Honda, *Nature*, 1972, **238**, 37–38.
16. G. Zhang, F. He, X. Zou, J. Gong, and H. Zhang, *J. Phys. Chem. Solids*, 2008, **69**, 1471–1474.
17. Y. Kim, S. Atherton, E. S. Brigham, and T. E. Mallouk, *J. Phys. Chem.*, 1993, **97**, 11802–11810.
18. T. Sasaki and M. Watanabe, *J. Phys. Chem. B*, 1997, **101**, 10159–10161.
19. P. Griesmar, G. Papin, C. Sanchez, and J. Livage, *Chem. Mater.*, 1991, **3**, 335–339.
20. J. Livage, M. Henry, and C. Sanchez, *Prog. Solid State Chem.*, 1988, **18**, 259–341.
21. T. Sugimoto, X. Zhou, and A. Muramatsu, *J. Colloid Interface Sci.*, 2003, **259**, 43–52.
22. R. Nedjar, M. M. Borel, and B. Raveau, *Mater. Res. Bull.*, 1985, **20**, 1291–1296.
23. Y. Matsumoto, *J. Solid State Chem.*, 1996, **126**, 227–234.
24. Q. Li, B. Guo, J. Yu, J. Ran, B. Zhang, H. Yan, and J. R. Gong, *J. Am. Chem. Soc.*, 2011, **133**, 10878–10884.
25. I. Lightcap, T. Kosel, and P. Kamat, *Nano Lett.*, 2010, **10**, 577–583.
26. T. Jaramillo, K. Jørgensen, J. Bonde, J. H. Nielsen, S. Hørch, and I. Chorkendorff, *Science (80-.)*, 2007, **317**, 100–102.
27. Q. Xiang, J. Yu, and M. Jaroniec, *J. Am. Chem. Soc.*, 2012, **134**, 6575–6578.
28. T. Jia, A. Kolpin, C. Ma, R. Chan, W.-M. Kwok, and S. C. E. Tsang, *Chem. Commun.*, 2014, **50**, 1185–1188.
29. Y. Hou, Z. Wen, S. Cui, X. Guo, and J. Chen, *Adv. Mater.*, 2013, **25**, 6291–6297.